Large-scale dynamics associated with clustering of extratropical cyclones affecting Western Europe

AGU PUBLICATIONS

JGR

Journal of Geophysical Research: Atmospheres

RESEARCH ARTICLE
10.1002/2014JD022305

Key Points:
- Analysis of physical mechanisms leading to cyclone clusters affecting Europe
- Recurrent extension of an intensified jet toward Europe leads to clustering
- Upstream secondary cyclogenesis is also strongly related to cyclone clustering

Supporting Information:
- Readme
- Figures S1–S8 and Table S1

Correspondence to:
J. G. Pinto,
j.g.pinto@reading.ac.uk

Citation:
Pinto, J. G., I. Gómara, G. Masato, H. F. Dacre, T. Woollings, and R. Caballero (2014), Large-scale dynamics associated with clustering of extratropical cyclones affecting Western Europe, *J. Geophys. Res. Atmos.*, *119*, 13,704–13,719, doi:10.1002/2014JD022305.

Received 12 JUL 2014
Accepted 20 NOV 2014
Accepted article online 25 NOV 2014
Published online 19 DEC 2014

Large-scale dynamics associated with clustering of extratropical cyclones affecting Western Europe

Joaquim G. Pinto[1,2], Iñigo Gómara[3], Giacomo Masato[1], Helen F. Dacre[1], Tim Woollings[4], and Rodrigo Caballero[5]

[1]Department of Meteorology, University of Reading, Reading, UK, [2]Institute for Geophysics and Meteorology, University of Cologne, Cologne, Germany, [3]Departamento de Geofísica y Meteorología and Instituto de Geociencias (IGEO), Universidad Complutense de Madrid, Madrid, Spain, [4]Atmospheric, Oceanic and Planetary Physics, Department of Physics, University of Oxford, Oxford, UK, [5]Department of Meteorology and Bert Bolin Centre for Climate Research, Stockholm University, Stockholm, Sweden

Abstract Some recent winters in Western Europe have been characterized by the occurrence of multiple extratropical cyclones following a similar path. The occurrence of such cyclone clusters leads to large socio-economic impacts due to damaging winds, storm surges, and floods. Recent studies have statistically characterized the clustering of extratropical cyclones over the North Atlantic and Europe and hypothesized potential physical mechanisms responsible for their formation. Here we analyze 4 months characterized by multiple cyclones over Western Europe (February 1990, January 1993, December 1999, and January 2007). The evolution of the eddy driven jet stream, Rossby wave-breaking, and upstream/downstream cyclone development are investigated to infer the role of the large-scale flow and to determine if clustered cyclones are related to each other. Results suggest that optimal conditions for the occurrence of cyclone clusters are provided by a recurrent extension of an intensified eddy driven jet toward Western Europe lasting at least 1 week. Multiple Rossby wave-breaking occurrences on both the poleward and equatorward flanks of the jet contribute to the development of these anomalous large-scale conditions. The analysis of the daily weather charts reveals that upstream cyclone development (secondary cyclogenesis, where new cyclones are generated on the trailing fronts of mature cyclones) is strongly related to cyclone clustering, with multiple cyclones developing on a single jet streak. The present analysis permits a deeper understanding of the physical reasons leading to the occurrence of cyclone families over the North Atlantic, enabling a better estimation of the associated cumulative risk over Europe.

1. Introduction

Extratropical cyclones generated in the North Atlantic storm track play a dominant role in determining the weather and climate of Western Europe. A comprehensive understanding of the controls on cyclone paths and characteristics is thus essential in order to interpret and predict the regional weather and climate [*Lamb*, 1991; *Neu et al*., 2013]. Cyclones are responsible for a large part of continental precipitation, with a contribution of 70–85% for Western and Central Europe in winter [*Hawcroft et al*., 2012], and they can cause wind damage and flooding both in coastal and inland areas [e.g., *Fink et al*., 2009; *Pfahl and Wernli*, 2012]. Intense extratropical cyclones are in fact the primary natural hazard affecting Western and Central Europe [e.g., *Della-Marta et al*., 2010; *Schwierz et al*., 2010; *Haylock*, 2011].

The winter of 2013/2014 in the North Atlantic and Europe was marked by the extremely frequent occurrence of cyclones, particularly in and around the British Isles. Over a period of about 2 months, this region was battered by a series of cyclones often occurring in quick succession and bringing strong winds, precipitation, and storm surges, leading to widespread property destruction and loss of life. Such a clustering of intense cyclones is not unprecedented: in 1990, Western Europe was affected by multiple cyclones from late January until early March [*McCallum and Norris*, 1990; *Lamb*, 1991]. Other historical cyclone clustering series occurred in 1993, 1999, and 2007 [e.g., *Ulbrich et al*., 2001; *Klawa and Ulbrich*, 2003; *Fink et al*., 2009]. Cyclone clusters are of particular concern for the insurance industry, as very high cumulative losses are incurred within the same season, placing great financial stress on insurers (insured losses due to the storm series of 1990, 1999, and 2007 were estimated at $10, $18, and $10 billion [*MunichRe*, 2010]).

Several recent studies have analyzed the serial clustering of extratropical cyclones from a statistical perspective [e.g., *Mailier et al*., 2006; *Vitolo et al*., 2009; *Pinto et al*., 2013; *Blender et al*., 2014]. These papers all show that serial clustering occurs more frequently over the eastern North Atlantic and Western Europe than would be expected by chance (Poisson process), suggesting that specific dynamical mechanisms may actively favor the occurrence of clusters. However, there has been little systematic investigation into the nature of such mechanisms so far. In this paper, we take a first step in this direction. We aim to characterize the large-scale atmospheric conditions associated with cyclone clustering and to explore how these conditions lead to this process. The following physical mechanisms have been conjectured in the literature in association with cyclone clustering [e.g., *Mailier et al*., 2006; *Hanley and Caballero*, 2012]: (i) the steering by the large-scale flow, (ii) secondary cyclogenesis of upstream developments on the trailing fronts of previous systems. Additionally, we consider a third hypothesis, (iii) downstream development of cyclones due to Rossby wave dispersion [*Simmons and Hoskins*, 1979].

The trajectories and intensity of extratropical cyclones over the North Atlantic and Europe are known to be affected by large-scale modes of variability, particularly the North Atlantic Oscillation [e.g., *Raible*, 2007; *Bader et al*., 2011; *Gómara et al*., 2014b]. For example, intense cyclones affecting Western Europe primarily occur when the eddy driven jet is (a) intensified and (b) extended toward Europe [*Pinto et al*., 2009; *Hanley and Caballero*, 2012]. Such conditions are typically associated with the occurrence of Rossby wave-breaking (RWB) on both sides of the jet, which intensifies the jet and constrains its location [*Hanley and Caballero*, 2012; *Gómara et al*., 2014a]. The relationship between the large-scale patterns (e.g., North Atlantic Oscillation) and cyclone clustering has been analyzed, e.g., by *Mailier et al*. [2006] using regression models. We hypothesize that the persistence of such large-scale conditions may lead to the steering and amplification of sequences of extratropical cyclones toward Western Europe.

Upstream growth of cyclones can lead to the occurrence of cyclone "families" (trains of cyclones with interrelated development). Such families can occur when multiple unstable waves develop and move rapidly along the trailing front in the wake of a large "parent" low [e.g., *Bjerknes and Solberg*, 1922], leading to secondary frontal cyclogenesis [e.g., *Parker*, 1998; *Rivals et al*., 1998]. Alternatively, cyclone families can be associated with downstream development, in which cyclogenesis occurs eastward of the parent cyclone due to Rossby wave dispersion [*Simmons and Hoskins*, 1979; *Chang*, 1993]. We aim to investigate the relationship between upstream and downstream development mechanisms in the formation of cyclone clusters.

In this paper, we employ an objective algorithm to detect clusters of extratropical cyclones in reanalysis data spanning the past three decades. We characterize the associated large-scale flow conditions, including jet intensity and location and Rossby wave-breaking activity. We then focus on four recent periods of cyclone clustering to study the specific mechanisms described above, namely, February 1990, January 1993, December 1999, and January 2007. Our goal in this exploratory study is not to definitively establish the dominance of any particular mechanism but rather to assess to what extent each mechanism is consistent with the observed behavior during these four periods.

The structure of the paper is as follows: Section 2 describes data and methods, while section 3 presents the selection of the periods of cyclone clustering. In section 4 the four selected months are evaluated in terms of jet intensity and location, cyclone tracks, and Rossby wave-breaking. Section 5 identifies the common features of the analyzed months in section 4 and presents a conceptual model of cyclone clustering. The summary and discussion section concludes the paper.

2. Data and Methods

The European Centre for Medium-Range Weather Forecasts Interim Re-Analysis (ERA-Interim) data set [*Dee et al*., 2011] is used. The horizontal resolution of the data set is T255 (approximately $0.75° \times 0.75°$ longitude/latitude), with 60 vertical levels from surface up to 0.1 hPa. The period considered is December to February 1980–2012 (at 6-hourly resolution).

In this study a two-dimensional RWB index from *Masato et al*. [2013a] is used, defined on the potential temperature (θ) on the dynamical tropopause (2 Potential Vorticity Units (PVU) $= 2 \times 10^{-6}$ K m^2 kg^{-1} s^{-1} surface). The temporal resolution of the index is daily (6-hourly θ fields are averaged into daily means) and the horizontal resolution is $4.5° \times 1.125°$ longitude/latitude. The index provides local-instantaneous occurrence

(*B* index) and direction of breaking (*DB* index) of large-scale RWB events (thin θ "streamers" are disregarded). The *B* index identifies regions where the mean meridional gradient of θ is reversed: if *B* is positive at a grid point, then RWB is detected at that location and time frame. Following *Gómara et al*. [2014a], no duration condition is imposed, as the focus is on instantaneous RWB. The *DB* index identifies the direction of breaking: positive and negative values of *DB* (above and below a threshold of +0.2 and −0.2) are identified as anticyclonic and cyclonic events, respectively. For further details on the RWB index, see *Pelly and Hoskins* [2003] and *Masato et al*. [2013a].

In order to identify single- and double-sided RWB events, a simple algorithm has been applied to daily two-dimensional maps (longitude versus latitude). For each day, the probability density function (PDF) of the latitude has been calculated for all grid points in the two-dimensional grid (40°W–10°E, 20°N–70°N) associated with a positive *B* index. A local maximum identification algorithm is then applied to identify the peaks of the distribution. If the distribution is bimodal, and both peaks are above a given threshold and apart by at least 20° in latitude, then the latitudes of these two peaks are retained as the locations of the double-sided RWB. If the distribution has only a single peak, the associated latitude is the location of the single-sided RWB. To exclude smaller RWBs, only the peaks exceeding a given threshold have been retained. The threshold is set as the total area underneath the PDF (i.e., the total number of *B* positive values) divided by the number of bins (i.e., the number of intervals along the *x* axis, which represents latitude values). In addition, the threshold for the single-sided RWB has been further multiplied by a factor of 5 in order to retain extensive single-sided breakings, which may likely influence the large-scale dynamics.

A cyclone identification and tracking algorithm [*Murray and Simmonds*, 1991] is applied to ERA-Interim (0.75° × 0.75°) 6-hourly data to obtain cyclone statistics over the North Atlantic (80°W–40°E, 30°N–75°N). Extratropical cyclones are identified based on the Laplacian of mean sea level pressure (MSLP) ($\nabla^2 p$), an approximation of the geostrophic relative vorticity of the system. An assignment algorithm is used to compile tracks considering the most probable trajectory of the cyclones between subsequent time frames. Basic properties of the cyclone life cycles are thus obtained (e.g., the evolution of core pressure and propagation velocity). The methodology has been adapted for Northern Hemisphere cyclone characteristics and compares well with other cyclone identification and tracking methodologies [*Pinto et al*., 2005; *Neu et al*., 2013]. Following *Pinto et al*. [2009], developing cyclones are selected when they verify: (i) cyclone lifetime $\geq$ 24 h; (ii) minimum MSLP $<$ 1000 hPa; (iii) maximum $(\nabla^2 p) > 0.6$ hPa degree latitude^{-2}; and (iv) maximum $\frac{\mathrm{d}}{\mathrm{d}t}\nabla^2 p \geq 0.3$ hPa degree latitude^{-2} d^{-1}. The minimum MSLP of the cyclone surface center is used as indicator of intensity in this study (cf. section 3 for further information).

Zonal and meridional wind components are used at 00 UTC of each day to analyze the position and intensity of the North Atlantic eddy driven jet. Following *Woollings et al*. [2010], the jet location is based on daily mean 850 hPa zonal wind. This choice of vertical level for the diagnostic enables a clear separation between the eddy driven jet (which extends throughout the depth of the troposphere) and the subtropical jet (which is confined to the upper troposphere). In order to focus on the eastern North Atlantic and Western Europe, the wind is averaged over the longitudes between 40°W and 10°E. The resulting field is subsequently low-pass filtered (Lanczos, 10 day cutoff frequency) and the latitudinal location of the maximum westerly wind speed is taken [cf. *Woollings et al*., 2010]. Note that jet indices computed using 925–700 hPa provide very similar results. The choice of 40°W–10°E is justified by the focus on cyclones affecting Western Europe. The anomalies of the jet intensity are calculated by subtracting the winter (December–February, DJF) 850 hPa long-term mean.

Available weather charts from the UK Met Office are used to analyze the influence of surface fronts and secondary cyclogenesis on clustering events. The frontal positions displayed in the frontal analysis charts are made by forecasters using (i) model and observed parameters such as temperature, wind shifts, dew point, cloud cover, cloud types, visibility, and lines in precipitation patterns and (ii) (post-2000 only) an automated frontal identification algorithm based on gradients of wet-bulb potential temperature [*Hewson*, 1997, 1998]. Thus, some subjectivity is present in the frontal analysis. To relate the frontal positions with reanalysis data, the frontal positions are reprojected onto a regular latitude/longitude grid. Historical storm names are obtained from the *Freie Universität* Berlin.

Finally, daily averaged *u* and *v* winds at 300 hPa (2.5° × 2.5°) from the National Centers for Environmental Prediction (NCEP) reanalysis data [*Kalnay et al*., 1996] are used for the Hövmoller diagrams (section 5).

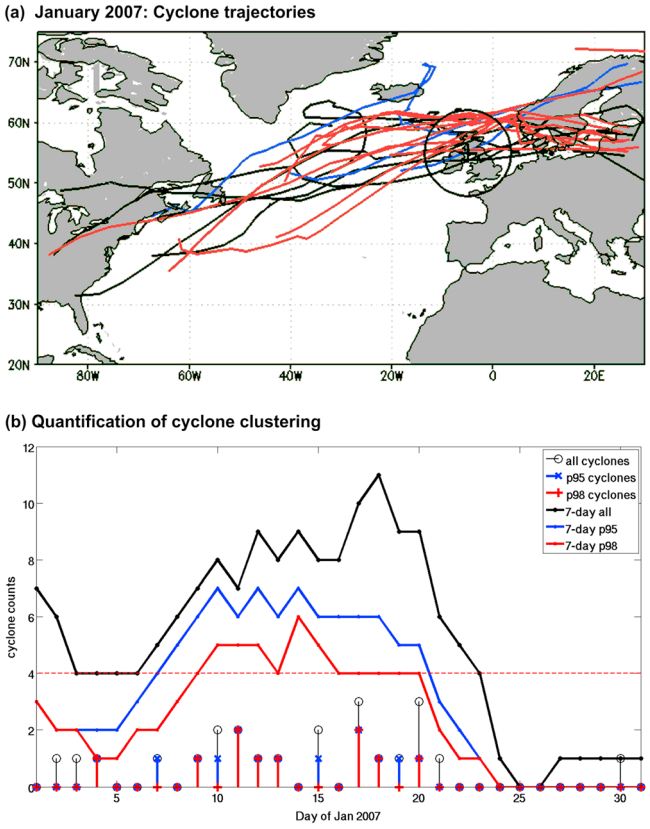

Figure 1. (a) Trajectories of all (black lines), p95 (blue lines), and p98 (red lines) cyclones crossing the circle detection area ((55°N, 5°W), $r = 700$ km) during January 2007. (b) All, p95, and p98 cyclone counts in January 2007 per calendar day (stems, see legend). Solid lines: 7 day running sums of cyclone counts. Dashed red line: threshold defined for clustering detection (four cyclones within 7 days).

3. Selection of Clustering Periods Within ERA-Interim

Identification of clustering events over Western Europe is carried out for the winter months (DJF 1980–2012). For this purpose, cyclone tracks are detected in a circular area covering the British Isles at the time where its location is nearest to the circle center (central position (55°N, 5°W), radius = 700 km). Figure 1a shows the detection area with the location of the January 2007 cyclone tracks overlaid. The cyclones tracking through the circular area are shown in three colors: red tracks indicate cyclones whose minimum core pressure within this area is below the climatological second MSLP percentile (p98 cyclones, 2% most intense) at (55°N, 5°W), blue tracks are cyclones whose core pressure is below the fifth percentile (p95, 5% most intense), and black tracks depict the remaining cyclones (all).

The method captures the majority of cyclones affecting the British Isles (Figure 1a). Further cyclones could easily be included if the area was slightly shifted south/north but obviously at the cost of losing other cyclones. The sensitivity of the results to the central position of the circular area (55°N, 5°W) has been investigated. Different locations between 45°N and 65°N with 5° increments along 5°W were tested and little difference in the major clustering periods was identified (not shown). Regarding the choice of radius (700 km), we have followed *Pinto et al.* [2013] which analyzed the sensitivity of the detection method to the choice of radius. Values between 400 and 1000 km were tested as this interval encompasses the typical range of effective radius for extratropical cyclones (computed following *Simmonds* [2000] and *Simmonds and Keay* [2000]). This range typically starts at 600 km and sometimes reaches 1000 km [*Rudeva and Gulev*, 2007]. *Pinto et al.* [2013] selected the value of 700 km as this choice of radius corresponds to a plateau of quasi-constant values of dispersion statistic (a measure of clustering), with small changes both to larger and smaller radii over most of the study area (their Figure S1).

In Figure 1b the daily counts of all, p95, and p98 cyclones in January 2007 are shown as stems. The occurrence of cyclone clustering events is quantified using a 7 day running sum of the daily counts (colored lines). A threshold of four or more consecutive cyclones within 7 days (dashed black line) is set to identify clustering periods.

Using these criteria, a period of 12 clustering days for p98 cyclones (9–20 January, red line) is identified, with a total of nine cyclones. If the criteria is used for p95 cyclones (blue line), the clustering period has a length of 14 days (7–20 January) including 14 p95 cyclones. For the other selected periods, either long clustering periods (e.g., 26 January to 5 February 1990 at the p95/p98 level) or multiple clustering periods (e.g., 6, 8–14, and 22–27 December 1999) are identified (see Table 1 for details). The values associated with the clustering periods (length, recurrence, and cyclones involved) are remarkable compared with climatology and rank among the top positions. Although January 1993 also presents above average values, cyclones over that

Table 1. Characterization of the Four Main Periods of Clustering[a]

	Clustering Periods		Length (Days)		Cyclone Counts per Event		Clustering Days per Month (%)	
	p95	p98	p95	p98	p95	p98	p95	p98
Jan 2007	7–20	9–20	**14**[4]	**12**[2]	**14**[3]	**9**[2]	**45.16**[4]	**38.71**[1]
Dec 1999	6		1		4		**45.16**[5]	19.35
	8–14		7		7			
	22–27	22–27	6	6	4	4		
Jan 1993	10–18	18	9	1	10	4	29.03	3.23
Feb 1990	26 Jan to 5 Feb	26 Jan to 5 Feb	**11**[9]	**11**[3]	**12**[5]	**12**[1]	**42.48**[6]	**24.78**[6]
	10	10	1	1	4	4		
	14	14	1	1	4	4		
	24 Feb to 2 Mar		7		6			
Climatology	Total 63	Total 43	6.03	4.46	6.86	5.46	13.16	6.65

[a]Top 10 rankings of clustering properties among each class (p95, p98 cyclones) during the whole base period (DJF 1980–2012) are highlighted in bolds and provided with superscripts. For more details, see text.

month mostly tracked further north and are thus not counted by the method. For p95 (p98) cyclones, the 1980–2012 winter long-term mean of the 7 day running sum is 1.36 (0.85) cyclones per week and the selected events represent approximately 13.16%—corresponding to 380 days (6.65%—corresponding to 192 days) of the total base period (2888 days). The total number of identified clustering events by the algorithm is 63 (43), which corresponds to 1.97 (1.34) per winter (DJF) season, with a mean length of 6.03 (4.46) days for p95 (p98) cyclones. The total number of p95 (p98) cyclones is 567 (355).

4. Characterization of Clustering Periods

The large-scale flow is analyzed during the four selected months (January 2007, December 1999, January 1993, and February 1990). In Figure 2, the jet stream latitude (black solid line) and speed anomalies (shadings) for the 850 hPa level averaged over the eastern North Atlantic (40°W–10°E) are shown. An intensified and quasi-stationary jet is observed for extended periods during each of the 4 months. This configuration is known to foster rapid intensification of individual cyclones affecting Europe [*Hanley and Caballero*, 2012; *Gómara et al*., 2014a], as the strong upward motion of air at the right-entrance and left-exit regions of the jet core seems to promote rapid storm amplification [e.g., *Uccellini*, 1990; *Rivière and Joly*, 2006a, 2006b]. In addition, the unusual persistence of the jet location (up to 2 weeks) and its positive speed anomalies (significant values in stippling) may foster the development of multiple cyclones and thus be related to the serial windstorm clustering over Western Europe, as conditions promoting strong cyclone intensification endure for long time periods.

The influence of RWB in modulating the jet state and promoting cyclone clustering is investigated in detail for the period 6–20 January 2007. This is illustrated in Figure 3, where daily fields of θ on the dynamical tropopause (2 PVU surface shadings; 00 UTC), jet intensity at 250 hPa (dashed contours; 00 UTC) and RWB occurrence ($B > 0$; hatched fields) are provided with p95 cyclone tracks overlaid (solid lines). When known, the names of the major cyclones are provided at the top of each subpanel.

During the period of 6–20 January 2007, a cluster of cyclones (Franz, Gerhard and Hanno; 9–13 January) is characterized by two strong and consecutive large-scale anticyclonic RWB episodes over the subtropical eastern North Atlantic. In particular, the second anticyclonic event (12 January) is accompanied by large-scale cyclonic RWB to the north of the jet. Two additional and smaller scale cyclonic RWB events (likely associated with Cyclones Gerhard and Franz, respectively) can also be observed in the θ field south east of Greenland and west of Scandinavia on the same day (cf. Figure 3). These two small-scale RWB events exert some local influence on the northernmost part of the jet (not shown) but do not appear to be the main contributors of the current large-scale configuration. This is also the reason that we imposed a strict criterion on the identification of large-scale RWBs, which are particularly efficient in driving and constraining the westerly flow in the midlatitudes [*Orlanski*, 2003].

Next, a period of single-sided (poleward) RWB follows (13–16 January), and finally, a second cluster of cyclones (Kyrill and Lancelot; 17–20 January) also corresponds to two simultaneous large-scale RWBs (north cyclonic and south anticyclonic) which tighten the jet from both flanks and extend it toward Western Europe. For comparison purposes, a similar analysis is performed for the periods 22–30 December 1999 (Figure S1 in

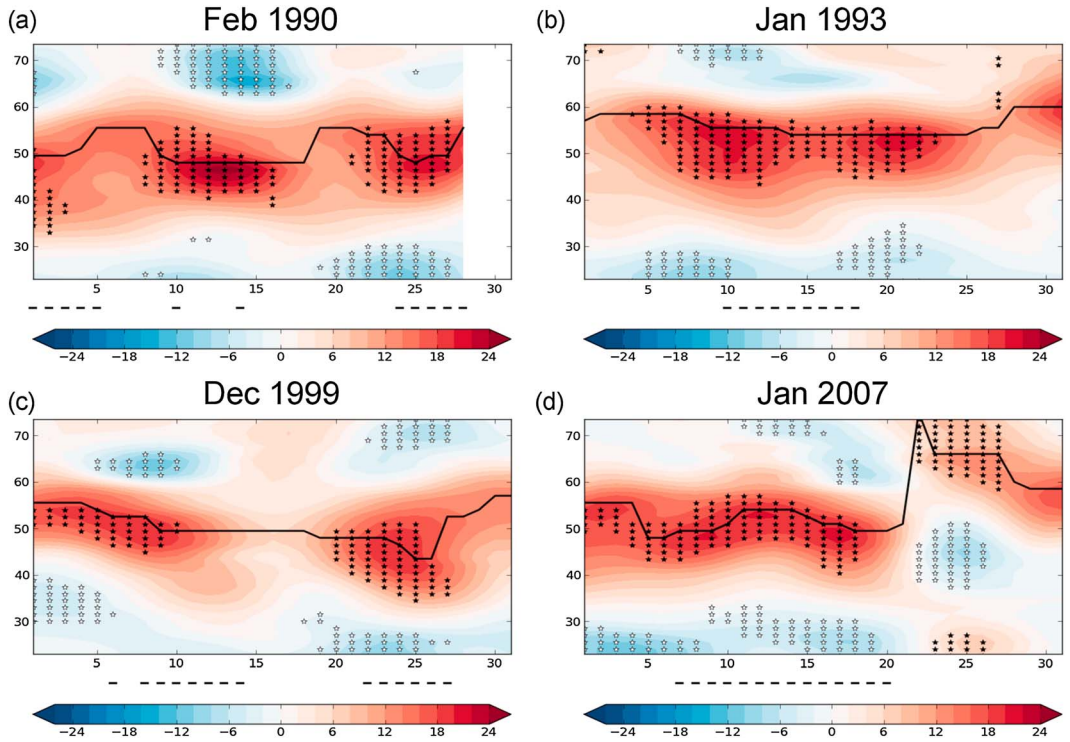

Figure 2. Jet stream (40°W–10°E) latitude (line, degrees north) and intensity at 850 hPa (colors, as anomalies to long-term mean in m s^{-1}) for February 1990, January 1993, December 1999, and January 2007, *x* axis corresponds to calendar days. Cyclone clustering periods (p95 cyclone counts) are marked by black dashed lines below each subpanel. Values above 90%/below 10% centiles are dotted (red dotted areas mean "jet significantly stronger than usual").

the supporting information), 1–30 January 1993 (Figure S2), and 1–28 February/1–2 March 1990 (Figure S3). These figures strongly suggest that the occurrence of strong, large-scale RWB events on both sides of the jet is a common feature in all clustering periods.

This phenomenon is quantified in Figure 4, where RWB amplitude (represented by the positive values in Figure 4) is averaged over (40°W–10°E) for the same periods, and the stippling indicates where the wave-breakings occur. The relative position of the RWB with respect to the jet location (black solid line) can also be inferred. For a large fraction of the considered 4 months, extensive RWB events are identified respectively to the north and to the south of the jet. The double-sided RWB periods show close correspondence to maximum positive jet speed anomalies (Figures 2a–2d). As an example, the RWB events in Figure 3 between 8 and 13 January and 16–20 January 2007 are well captured and lead to the intensified and quasi-stationary jet state reported above (Figures 2d and 4d). Nevertheless, it is important to note that the strong jet observed in Figures 2 and 4 (black solid line) is not completely stationary in time (see Figure 3 and Figures S1 to S3 for comparison), as the apparent quasi-stationarity arises from the time filtering of the wind data (cf. section 2). The recurrent occurrence of RWB events interacting with the jet at synoptic time scales (1 to 5 days) is the real cause for the emerging quasi-stationary.

Figure 5 shows the basic properties of the 850 hPa jet conditional on the occurrence of single- and double- sided RWB events and cyclone clustering for the whole reanalysis period. In Figures 5a and 5b the jet speed at 850 hPa and jet latitude probability density functions are composited considering the daily values of the two-sided RWB events. The uncertainty range is derived using a Monte Carlo method, with 100 simulations randomly extracting the data from each subsample, respectively. The total number of days considered for the long-term distribution (red) is 2876, from which 452 days exhibit double-sided RWBs (blue distribution), while the remaining 2424 do not exhibit double-sided RWB (green distribution). When compared against the climatology and nondouble-sided RWB events, the double-sided RWB events are

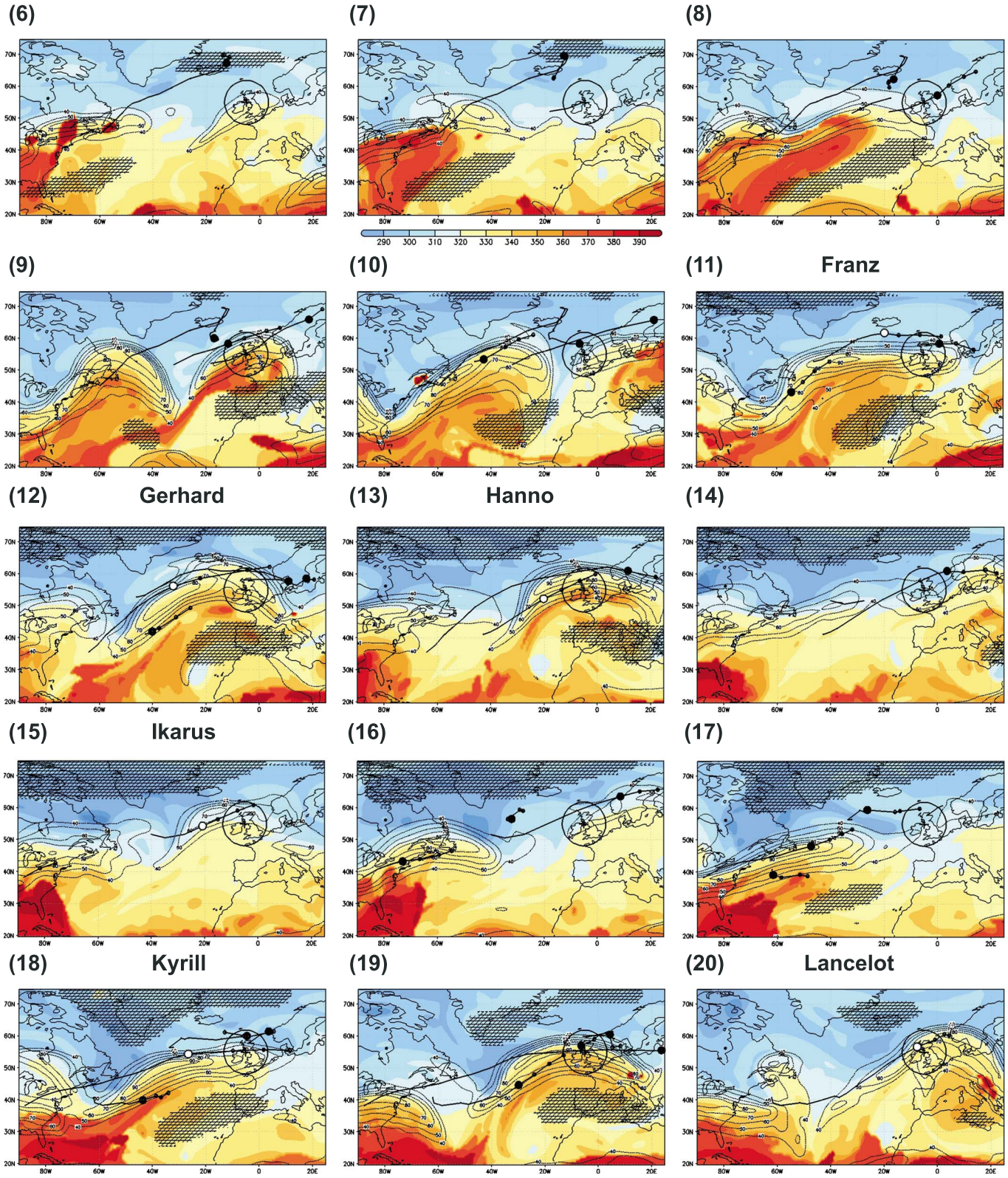

Figure 3. 6–20 January 2007. Red/blue shadings: θ on the 2 PVU surface in K (00 UTC). Hatched fields: daily RWB occurrence. Dashed contours: wind intensity at 250 hPa (m s^{-1}, 00 UTC), contours drawn from 40 m s^{-1} with 10 m s^{-1} contour intervals. Solid contour lines: Full p95 cyclone trajectories until 18 UTC of each day. Large filled black dots: Cyclone positions at 00 UTC. Small circles: three forthcoming cyclone positions on the same date. Large open white dots: Positions (00 UTC) of named historical storms crossing the detection area ((55°N, 5°W), r = 700 km) on that day.

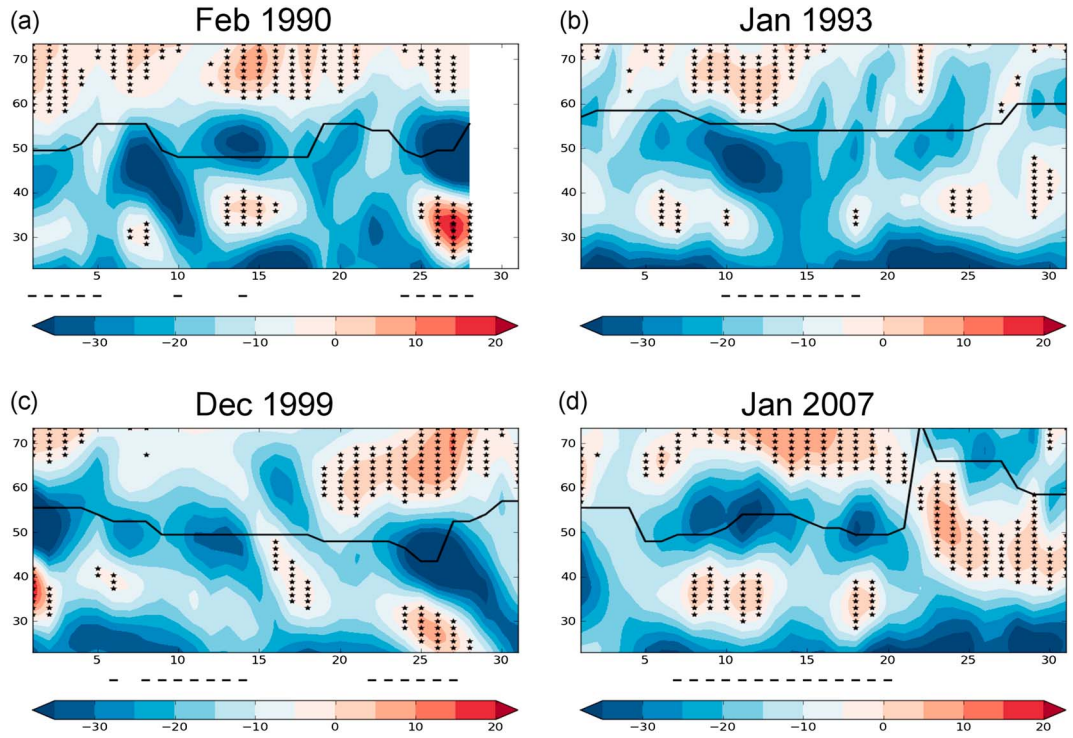

Figure 4. Jet stream (40°W–10°E) latitude (line, degrees north) for February 1990, January 1993, December 1999, and January 2007, the *x* axis corresponds to calendar days (as in Figure 2) and cyclone clustering periods (p95 cyclone counts) are marked by black dashed lines below each panel. The colors show the RWB amplitude (represented by positive values) averaged over (40°W–10°E). The black stippling indicates where the wave-breakings occur (see the text for more details).

associated with a stronger and more latitudinally constrained jet over Western Europe. Differences are up to 6 m/s and point to a more limited corridor for the jet location (45°N–55°N). Given the typical location for the occurrence of cyclonic (anticyclonic) RWB poleward (equatorward) of the eddy driven jet [e.g., *Gómara et al.*, 2014a, Figures 1c and 1d], it is natural that the jet stream over the eastern North Atlantic is constrained within these latitudinal bounds if double-sided RWB occur.

In the lower panels (Figures 5c and 5d), the jet characteristics associated with the occurrence of clustering of p95 cyclones over the British Isles (55°N, 5°W) are illustrated (cf. section 3 and Figure 1). In general, the jet speed and latitudinal extent associated with these cyclones (380 of 2876 total days) are very similar to those of the double-sided RWB described above, which suggests a strong relationship between double-sided RWB and cyclone clustering. It should be pointed out that the two subsets are not entirely overlapping, as only 44% of the total storm clustering days are also characterized by the occurrence of the double-sided RWB. For this calculation a 2 day lead or lag between cyclone clustering and RWB dates is allowed (i.e., if within a 5 day period there is at least 1 day characterized by a two-sided RWB and 1 day characterized by cyclone clustering, then the central day of the period is labeled as a two-sided RWB). Also, the 29 February of every year are disregarded (thus the base period is here 2876 days instead of 2888 days). From the remaining 56%, 21% are characterized by one-sided RWB and 35% by no RWB (see Table S1). When considering the stronger (p98) cyclones as input, the number of overlapping dates increases from 44% to 48%, and the anomalous jet conditions are amplified (Figure S4 and Table S1). Here 20% of the remaining cases are characterized by one-sided RWB and 32% by no RWB. On the contrary, when considering the whole base period (DJF 1980–2012), the days without RWB clearly dominate (61% of days), and days with two-sided RWB events become rarer (16%, cf. Table S1). These numbers, together with the results in Figure 5, highlight the strong connection between double-sided RWB and cyclone clustering.

Some attention should also be paid to the effect that the clustering method itself introduces in the distributions in Figure 5. As the area of selection is a circle of 700 km radius, one might expect that the jet location (blue distribution in Figure 5d) is highly constrained around its center (55°N). According to *Mahlstein et al.* [2012], a jet

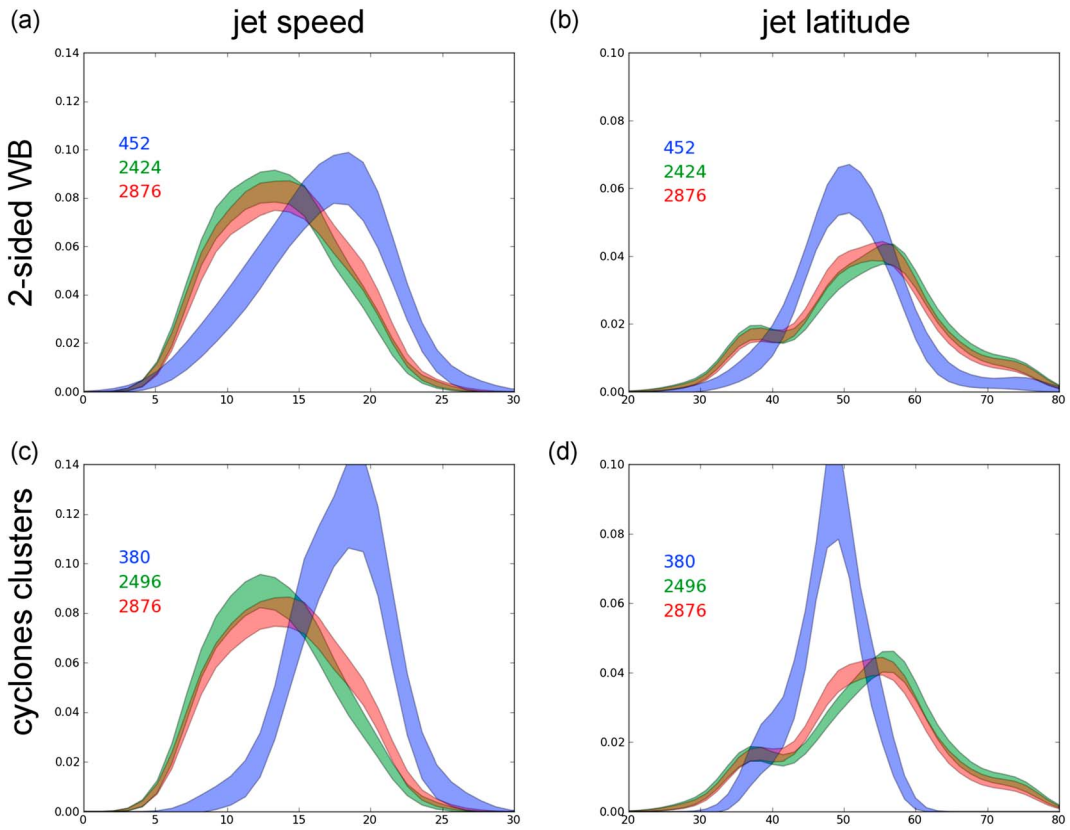

Figure 5. (a, b) Comparison for distributions with two-sided RWB (blue) versus other cases (green) and all cases (red) for low-pass filtered jet speed at 850 hPa (m s^{-1}) and jet latitude (degrees north), all for (40°W–10°E). (b, d) Same as above but for the occurrence of p95 cyclone clusters intercepting the detection area across the British Isles (55°N, 5°W). The uncertainty of the PDFs reflects the size of the data set it is associated with.

stream located around this latitude is associated with a higher chance of strong winds over the southern half of the British Isles, France, and Benelux countries. A sensitivity analysis for other latitudes than 55°N leads to comparable results for the latitude constraint, but with a slightly shifted peak of the jet distribution (not shown).

Figure 6 shows the vertical structure of the jet associated with cyclone clustering. The vertical cross section (1000–150 hPa) of the climatological jet averaged over (40°W–10°E) is shown in Figure 6a. The analogous composite for the jet associated with clustering of p95 cyclones is provided in Figure 6b and reveals very intense and latitudinally constrained upper level winds centered at 50°N with a strong signature at lower levels. In Figure 6c, the associated composite anomalies are calculated by subtracting the long-term mean. A very robust and barotropic jet structure is present at all pressure levels during clustering of p95 cyclones (5 and 95% confidence intervals in dashed contours using a Monte Carlo test of 1000 random iterations). Whereas positive anomalies are constrained around 45°N–50°N, negative anomalies are found in the ranges 25°N–30°N and 60°N–80°N. If more intense (p98) cyclones are considered, the positive jet anomalies are even stronger and more latitudinally constrained (Figure 6d). As suggested in previous studies [*Pinto et al.*, 2009; *Gómara et al.*, 2014a], a more intense jet over the eastern North Atlantic is related to enhanced baroclinicity both at upper and at lower levels and is consistent with increased storm activity.

5. Cyclone Clusters and Cyclone Families

In the previous section we have demonstrated the relationship between the large-scale flow conditions and cyclone clusters. In particular, the presence of an intense and persistent eddy driven jet is related to the occurrence of cyclone clusters over Western Europe. In this section, we investigate the relationship between selected cyclones over the Northeast Atlantic region (35°N–70°N, 15°W–20°E) within each cyclone cluster. This is done in order to enable the analysis of European windstorms following a similar path out of the

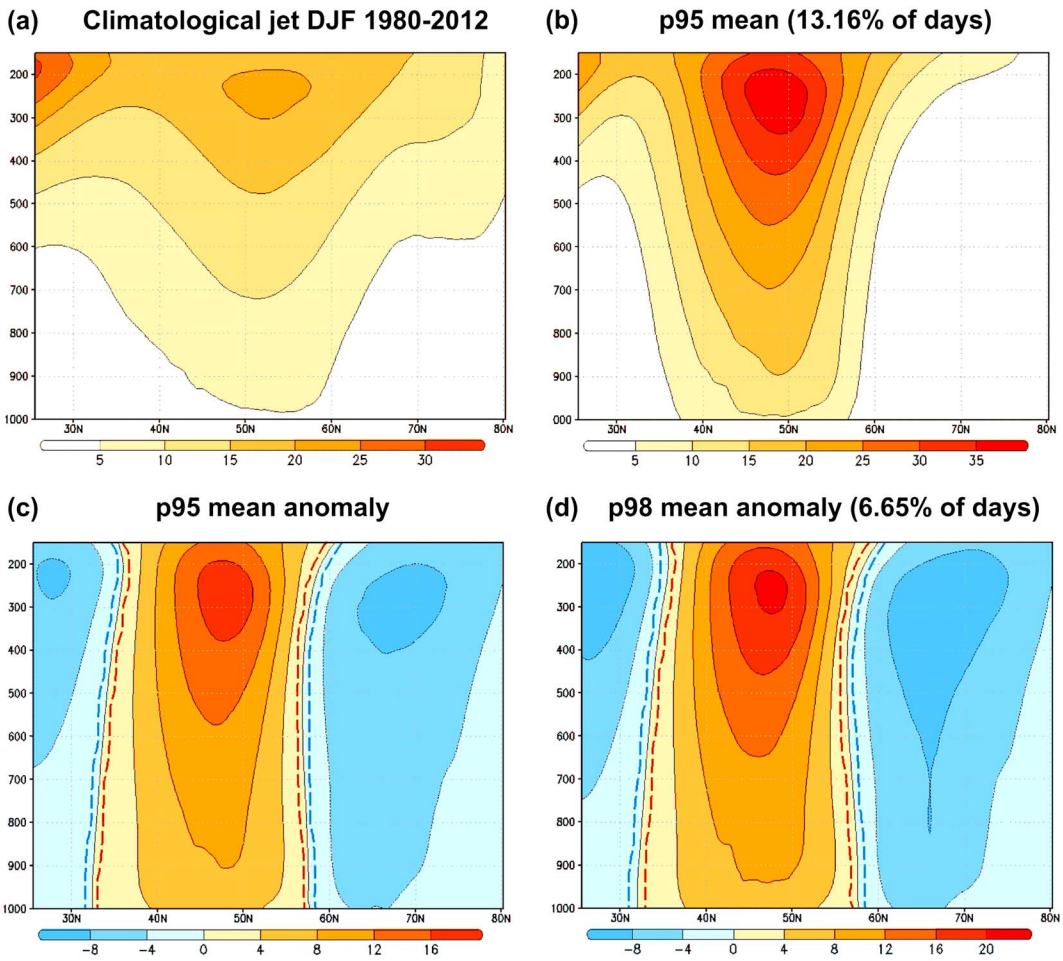

Figure 6. (a) Climatological jet (daily means): 1000 to 150 hPa pressure levels averaged over (40°W–10°E) in m s^{-1}; DJF 1980–2012. (b) Composite wind intensity during clustering dates of p95 cyclones on grid point (55°N, 5°W). (c) Same as Figure 6b but for the composite anomalies subtracting climatology. Marked with dashed red/blue contours are 5 and 95% Monte Carlo intervals (1000 random iterations). (d) Same as Figure 6c but for p98 cyclones.

detection area (e.g., Lothar and Martin, 25–28 December 1999; cf. section 3). We consider two mechanisms for linking the cyclones: (i) Upstream development of cyclones (secondary frontal cyclogenesis [e.g., *Parker*, 1998]), in which new cyclones are generated, e.g., on the trailing (cold) fronts of mature cyclones and (ii) downstream development of cyclones [e.g., *Simmons and Hoskins*, 1979], in which new cyclones form downstream (i.e., eastward) of existing cyclones due to Rossby wave dispersion.

Rather than attempting a climatological investigation, in this section we look for evidence of these two mechanisms in the 4 months focused on in this paper. The identification of a specific mechanism is contrasted with the null hypothesis that the development of cyclones within a cluster is mutually unrelated, even if they occur in quick succession, other than through the fact that they develop under the same strong, persistent, upper tropospheric jet.

Secondary frontal cyclones develop on the trailing fronts of preexisting cyclones. Although many observational and theoretical modeling studies have been carried out on the structure and evolution of secondary frontal cyclones, there is no objective method of differentiating them from other types of cyclones [*Parker*, 1998]. In general, primary frontal cyclones develop in large-scale baroclinic regions such as the polar frontal zone, where strong temperature gradients separate cold air of polar origin from tropical air. They have a typical life cycle of 3–4 days and a horizontal scale ~2000 km. Secondary frontal cyclones typically develop in more localized baroclinic regions such as the trailing cold fronts of preexisting frontal cyclones. They tend to be smaller in scale and develop over 1–2 days. Compared to primary cyclones, their

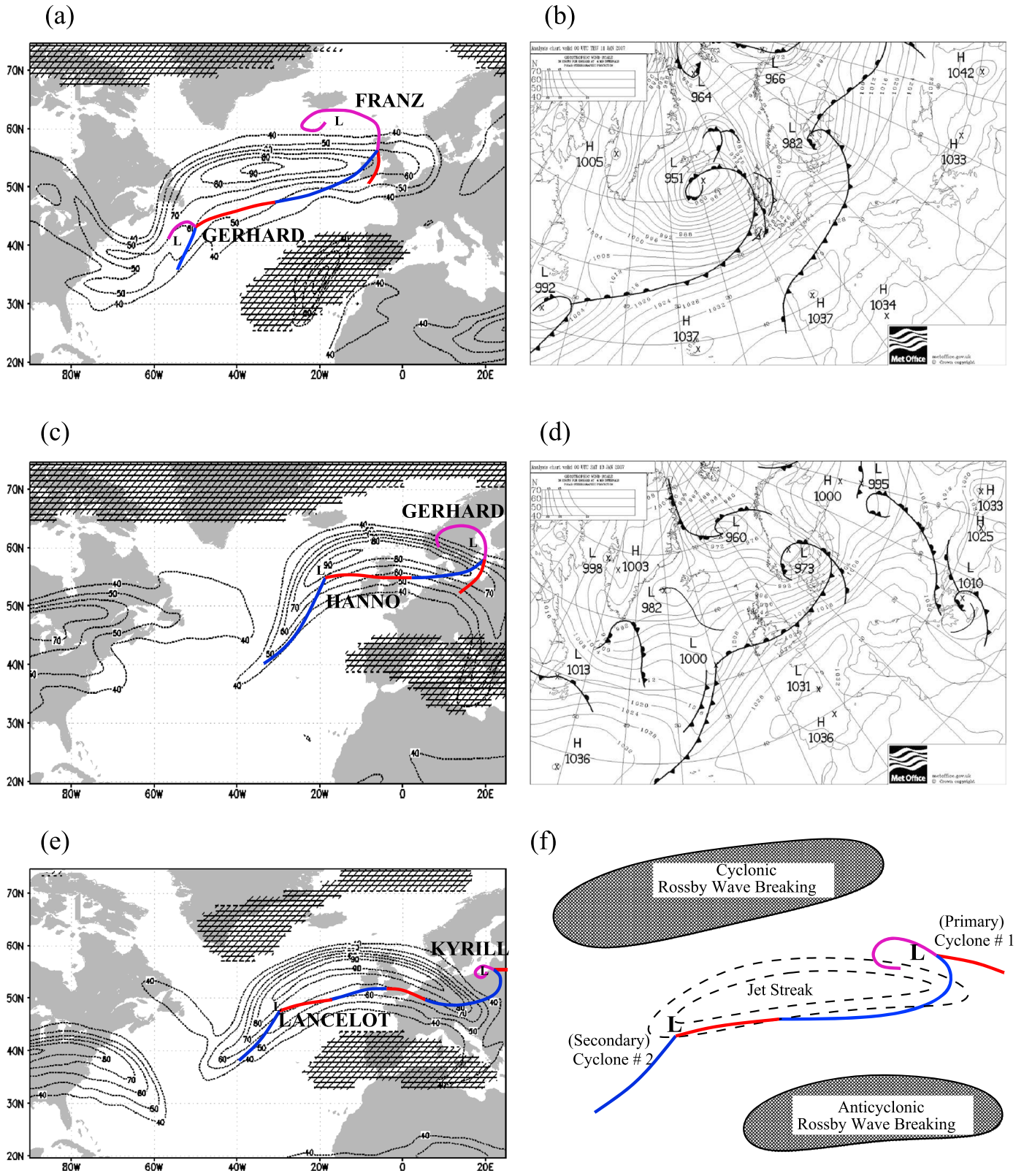

Figure 7. (a, c, and e) RWB occurrence ($B > 0$; hatched), wind intensity at 250 hPa (m s^{-1}; dashed contours drawn from 40 m s^{-1} with 10 m s^{-1} contour intervals), cyclone surface centers and fronts (from UK Met Office weather charts; red/blue/purple solid lines for warm/cold/occluded fronts) for 00 UTC on example dates 11, 13, and 19 January 2007. (b, d) Weather charts (00 UTC) on 11 and 13 January 2007. (f) Schematic summary showing relative positions of clustering cyclones with respect to jet streak location and location of RWB.

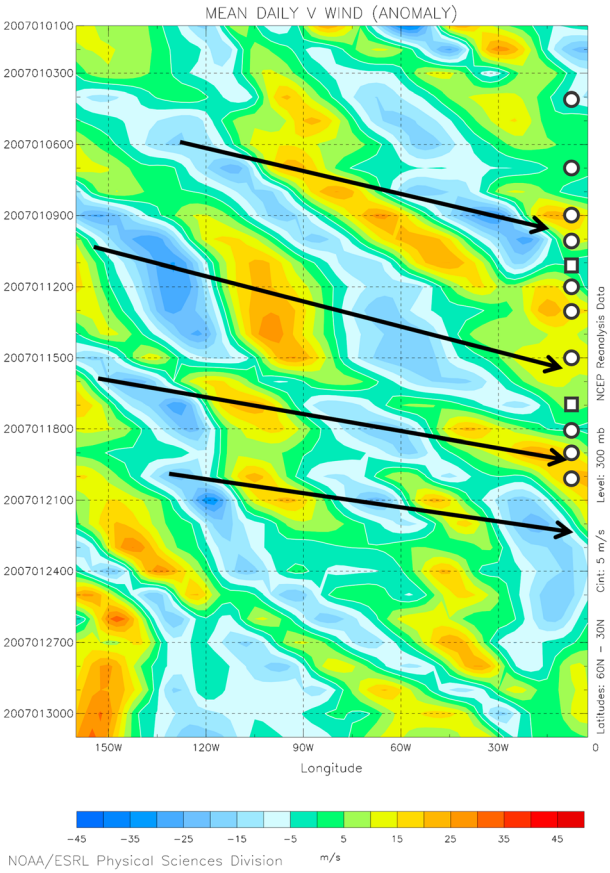

Figure 8. Hovmöller diagram of zonal wind daily speed anomalies at 300 hPa (m s^{-1}) for January 2007, averaged over latitude band to (30°N–60°N). The black arrows give subjective indications of the group velocity of some Rossby wave packets. Counts of p95 cyclones per day (see Figure 1a) crossing the meridian 5°W are provided in geometric forms (circles: one count per day; squares: two counts per day).

development is thought to be more influenced by nonbaroclinic mechanisms such as large-scale strain [*Dritschel et al.*, 1991; *Bishop and Thorpe*, 1994a, 1994b; *Renfrew et al.*, 1997; *Dacre and Gray*, 2006], frontal shear [*Chaboureau and Thorpe*, 1999; *Joly and Thorpe*, 1991], latent heat release [*Joly and Thorpe*, 1990; *Schär and Davies*, 1990; *Plant et al.*, 2003], and boundary layer friction [*Adamson et al.*, 2006]. In this paper, secondary cyclones are defined as those which develop on the trailing cold front of preexisting cyclones (as depicted on the UK Met Office frontal analysis charts).

To investigate upstream secondary frontal cyclone development, we replot Figure 3 retaining only 250 hPa wind speed and areas of RWB and add the surface central positions and fronts of cyclones as identified in daily weather charts from the UK Met-Office. Examples of such charts are presented in Figure 7, which depicts the dates 11, 13, and 19 January 2007. Cyclone names are added, and only those fronts associated with cyclones tracking over Western Europe are shown in Figure 7. In all three cases, a jet streak feature links two cyclones, with a "parent" cyclone in the left-exit region of the jet, typically already occluding (e.g., Franz in Figure 7a), while a new secondary cyclone is developing in the right-entrance region of the jet (Gerhard in the same figure). Two days later (Figure 7c), cyclone Gerhard is the occluding parent cyclone, while a new storm (Hanno) is developing in the right-entrance region of the jet streak. The pattern occurs again on the 19 January 2007 (Figure 7e), with Kyrill as a parent cyclone and Lancelot as a secondary cyclone. In all these cases, cyclonic wave-breaking is identified on the poleward side of the jet (typically northwestward), while anticyclonic wave-breaking is located on the equatorward side of the jet (typically located southeastward). The analysis of similar charts for the other 3 months studied (see Figures S5 to S7) suggests a similar pattern of upper and lower level features and thus leads to the conceptual model shown in Figure 7f. As expected from the literature [e.g., *Uccellini*, 1990], cyclones are typically generated in the right-entrance region of the upper level jet and travel toward the left-exit region. The anomalously strong upper level jet streak is related to strong wind shear and strong low-level temperature gradients through thermal wind balance, thus maintaining the high baroclinicity necessary for explosive cyclone growth. Thus, it appears that the individual cyclones within the clusters examined can be related via the upstream development mechanism. This means that secondary cyclones form upstream, on the trailing cold fronts of primary cyclones, and develop into mature cyclones following the same path.

We now investigate the possibility that the process of downstream development enhances the clustering of cyclones by enabling several cyclones to develop in rapid succession. Downstream development is a feature of the dispersive nature of Rossby wave packets [*Simmons and Hoskins*, 1979]. Relative to the surface, the group velocity of synoptic-scale wave packets is directed eastward and is faster than the phase velocity. This means that existing cyclonic and anticyclonic anomalies move eastward over the surface but new anomalies develop downstream, or further east, of these as the wave energy disperses. Hence, the development of several cyclones can be linked, with new cyclones forming downstream of their parent.

To investigate this mechanism, we have followed *Chang* [1993] in generating Hovmöller diagrams of 300 hPa meridional wind anomalies for the four winters. The diagram for January 2007 is presented in Figure 8 as an example. Note that the meridional wind has been averaged over the 30°N–60°N band of latitude, so this picture illustrates synoptic and large-scale features of the flow only. The Hövmoller shows several clear Rossby wave trains with the characteristic signature of a group velocity (indicated by black arrows) which is faster than the phase velocity at which individual wind anomalies propagate. These wave packets arrive at the Greenwich meridian between 11 and 21 January (see Figure 8), which suggests that downstream development may have played a role in the development of some of these cyclones. It is interesting to note that during this core period of clustering, phase speeds in the western and central North Atlantic are in fact close to zero (albeit interspersed with some propagation), suggesting that stationary wave activity (i.e., which does not propagate downstream) may play an important role in controlling such events. However, the occurrence of multiple cyclones over Europe does not correspond to the arrival of several cyclones from the same wave packet. This is because multiple cyclones from the same wave packet do not last long enough to cross the same meridian. The wavelength of the packets in Figure 8 is typically 4000 km (in agreement with *Chang and Yu* [1999]), yet individual anomalies typically progress eastward by only around 2000 km during their lifetime.

Analysis of the other 3 months supports this result, that the clustering of European cyclones cannot generally be linked to the arrival of several cyclones from the same Rossby wave packet. As in the null hypothesis, the intense, straight jet stream provides a favorable waveguide for the wave packets but the packets themselves may not be dynamically linked. Still, downstream development is a mechanism for cyclone growth which may have played a role in the development of some, if not all, of the individual cyclones during these anomalous seasons. This applies particularly for the first cyclones of a storm series. For example, in the December 1999 case (Figure S8), clear wave packets arrive at the Greenwich meridian around 23 and 30 of December. The period of cyclone clustering lies between these dates, suggesting that downstream development may have played a role in the early cyclones of the cluster but not in the later ones.

6. Summary and Discussion

Four winter months corresponding to the main periods of the cyclone series of 1990, 1993, 1999, and 2007 were analyzed to identify the physical mechanisms associated with their occurrence. Our results identify during these clustering episodes a recurrent extension of an intensified eddy driven jet toward Western Europe which endures at least 1 week. On a daily basis, this corresponds to the occurrence of multiple jet streak events which successively occupy this location over several weeks. Cyclonic and anticyclonic Rossby wave-breaking events to the north and south of the eddy driven jet contribute to its recurring intensification and extension toward Europe and constrain the location of the jet typically within a limited corridor around 50°N. As a consequence, the large-scale conditions promoting rapid cyclone intensification persist for long time periods and increase the likelihood of storm clustering. Our results clearly document the importance of the steering by the large-scale flow for cyclone clustering.

Regarding the interrelated behavior between RWB occurrence and the jet state, it is well known that preferred locations of wave-breaking occurrence are located to the north (cyclonic) and south (anticyclonic) flanks of the eddy driven jet due to horizontal wind shear at upper levels [*Gabriel and Peters*, 2008]. The reverse effect—RWB as a cause of the changes in the mean flow, sometimes represented by the North Atlantic Oscillation—has also been described in various studies [e.g., *Franzke et al*., 2004; *Benedict et al*., 2004; *Rivière and Orlanski*, 2007; *Strong and Magnusdottir*, 2008b; *Michel and Rivière*, 2011]. In particular, the growth and decay of the positive phase of the North Atlantic Oscillation, which projects onto the large-scale configuration fostering clustering over the UK (cf. *Gómara et al*. [2014b]; Figure 2), is suggested to be forced by Rossby wave trains traveling from the North Pacific into the North Atlantic [*Feldstein*, 2003; *Strong and Magnusdottir*, 2008a]. Visual inspection of Figures 3 and S1–S3, corroborates with this argument, as RWB occurrence appears to steer the jet configuration. For predictability purposes, the variability and origin of these waves is undoubtedly an interesting path for future research.

An intensified eddy driven jet (as identified in the 4 months studied here) is associated with enhanced vertical wind shear and hence baroclinicity at lower levels, thus increasing the probability of explosive growth of baroclinic disturbances [*Hoskins et al*., 1985; *Gyakum and Danielson*, 2000; *Dacre and Gray*, 2013]. In the traditional view, cyclones themselves present two different life cycle behaviors depending on their

contrasting upper air evolution during their decaying stage (LC1 - anticyclonic and LC2 - cyclonic [e.g., *Thorncroft et al*., 1993]), and develop under a single jet streak. In the examples studied here, jet streaks are generated by previous and unrelated Rossby wave trains with greater temporal and spatial scales than those local RWB events related to the cyclones themselves [*McIntyre and Palmer*, 1983; *Nakamura and Wallace*, 1993]. Such upper level waves interacting with the jet stream may lead to the creation of multiple jet streaks (e.g., Figure 3), each favoring rapid cyclone intensification [*Reed and Albright*, 1986]. In fact, the strong divergence in the right-entrance and left-exit regions of a jet streak further contributes to enhance cyclone growth [*Uccellini*, 1990; *Rivière and Joly*, 2006a, 2006b]. These large-scale conditions analyzed here are thus consistent with the occurrence of multiple intense cyclones.

Additionally, this study highlights the importance of cyclone families and secondary cyclogenesis, particularly of upstream developments on trailing cold fronts of preexisting mature cyclones. The manual analysis of frontal developments has allowed the establishment of a link between cyclones based on synoptic plausibility and causality. A recurring pattern is identified, in which a developing cyclone is located in the right-entrance region of the jet on the trailing front of a mature cyclone located in the left-exit region of the same jet streak (Figure 7). The new cyclone follows a similar path to the previous cyclone toward the poleward side of the jet streak. This evidence is consistent with the idea of cyclone families and secondary cyclogenesis [e.g., *Bjerknes and Solberg*, 1922; *Parker*, 1998]. In fact, many of the top ranking destructive cyclones affecting Western Europe are secondary cyclones developing in the Northeast Atlantic region [e.g., *Dacre and Gray*, 2009].

The possible role of downstream development associated with the dispersive nature of Rossby waves [*Simmons and Hoskins*, 1979] was also analyzed. While this process can lead to cyclone development to the east of the parent cyclone [e.g., *Chang and Yu*, 1999; *Riemer et al*., 2008], it cannot explain the cyclone clustering periods presented here. While Rossby wave packets are present during these periods, the wavelengths are too long to correspond to the different cyclones within the clustering families.

This exploratory study provides the first dynamical analysis of the occurrence of clusters of extratropical cyclones over the North Atlantic, focusing on the role of secondary cyclogenesis and jet dynamics, and thus permitting a better understanding of the physical mechanisms leading to the occurrence of such cyclone families. The robustness of these results should be tested in a more complete analysis for the whole reanalysis period, and on other case studies like the winter of 2013/2014, in which a cyclone series led to severe impacts particularly in the United Kingdom. An interesting question which remains to be investigated concerns the relative roles played by the synoptic-scale temperature gradient associated with the jet streak and the mesoscale temperature gradient associated with the trailing cold front of the primary cyclone in determining the rate of secondary cyclone development. In addition, a more detailed analysis quantifying the role of deformation strain, shear, and latent heat release (all thought to be important for secondary cyclone development) could be performed to further characterize the relationship between cyclone clustering and secondary cyclogenesis. Other possible lines of future research are the estimation of the implications of cyclone clustering to the seriality of windstorm losses [e.g., *Karremann et al*., 2014], and the analysis of the identified mechanisms of cyclone clustering in high-resolution general circulation models like the High-Resolution Global Environmental Model [*Shaffrey et al*., 2009] to enable a better understanding of the projected changes of cyclone clustering under future climate conditions [*Pinto et al*., 2013]. With this aim, the representation of Rossby wave-breaking and its interactions with the upper level jet in general circulation models [e.g., *Masato et al*., 2013b] are of particular interest.

Acknowledgments

We thank the European Centre for Medium-Range Weather Forecasts and the National Centers for Environmental Prediction for the reanalysis data ERA-Interim and NCEP. We also thank the UK Met Office for the weather charts and the *Freie Universität* Berlin for the storm names. Iñigo Gómara is supported by Spanish national funds (research project MULCLIVAR CGL2012-38923-C02-01). We thank Sven Ulbrich (University of Cologne) and Marc Stringer (University of Reading) for help with data processing. We are grateful to John Methven, Len Shaffrey (both University of Reading), and David Stephenson (University of Exeter) for discussions and Peter Clark (University of Reading) for providing additional synoptic charts. We also thank Olivia Martius and two anonymous reviewers for their helpful and constructive comments. The ERA-Interim Re-analysis data set is available from European Centre for Medium-Range Weather Forecasts (http://apps.ecmwf.int/datasets/). The NCEP reanalysis data set is available from the National Centers for Environmental Prediction (www.ncep.noaa.gov/). The weather charts are available from the UK Met Office (http://www.metoffice.gov.uk), and the storm names from the *Freie Universität* Berlin (http://www.met.fu-berlin.de/adopt-a-vortex/). All other data are available from the authors (j.g.pinto@reading.ac.uk).

References

Adamson, D. S., S. E. Belcher, B. J. Hoskins, and R. S. Plant (2006), Boundary layer friction in mid-latitude cyclones, *Q. J. R. Meteorol. Soc.*, *132*, 101–124.

Bader, J., M. D. S. Mesquita, K. I. Hodges, N. Keenlyside, S. Østerhus, and M. Miles (2011), A review on Northern Hemisphere sea-ice, storminess and the North Atlantic Oscillation: Observations and projected changes, *Atmos. Res.*, *101*, 809–834.

Benedict, J. J., S. Lee, and S. B. Feldstein (2004), Synoptic view of the North Atlantic Oscillation, *J. Atmos. Sci.*, *61*, 121–144.

Bishop, C. H., and A. J. Thorpe (1994a), Frontal wave stability during moist deformation frontogenesis. Part I: Linear wave dynamics, *J. Atmos. Sci.*, *51*, 852–873.

Bishop, C. H., and A. J. Thorpe (1994b), Frontal wave stability during moist deformation frontogenesis. Part II: The suppression of non linear wave development, *J. Atmos. Sci.*, *51*, 874–888.

Bjerknes, J., and H. Solberg (1922), Life cycle of cyclones and the polar front theory of atmospheric circulation, *Geofys. Publ.*, *3*, 3–18.

Blender, R., C. C. Raible, and F. Lunkeit (2014), Non-exponential return time distributions for vorticity extremes explained by fractional Poisson processes, *Q. J. R. Meteorol. Soc.*, doi:10.1002/qj.2354.

Chaboureau, J. P., and A. J. Thorpe (1999), Frontogenesis and the development of secondary wave cyclones in FASTEX, *Q. J. R. Meteorol. Soc.*, *125*, 925–940.
Chang, E. K. (1993), Downstream development of baroclinic waves as inferred from regression analysis, *J. Atmos. Sci.*, *50*, 2038–2053.
Chang, E. K., and D. B. Yu (1999), Characteristics of wave packets in the upper troposphere. Part I: Northern Hemisphere winter, *J. Atmos. Sci.*, *56*, 1708–1728.
Dacre, H. F., and S. L. Gray (2006), Life-cycle simulations of low-level frontal waves and the impact of deformation strain, *Q. J. R. Meteorol. Soc.*, *132*, 2171–2190.
Dacre, H. F., and S. L. Gray (2009), The spatial distribution and evolution characteristics of North Atlantic cyclones, *Mon. Weather Rev.*, *137*, 99–115.
Dacre, H. F., and S. L. Gray (2013), Quantifying the climatological relationship between extratropical cyclone intensity and atmospheric precursors, *Geophys. Res. Lett.*, *40*, 2322–2327, doi:10.1002/grl.50105.
Dee, D., et al. (2011), The ERA-Interim reanalysis: Configuration and performance of the data assimilation system, *Q. J. R. Meteorol. Soc.*, *137*, 553–597.
Della-Marta, P. M., M. A. Liniger, C. Appenzeller, D. N. Bresch, P. Köllner-Heck, and V. Muccione (2010), Improved estimates of the European winter windstorm climate and the risk of reinsurance loss using climate model data, *J. Appl. Meteorol. Climatol.*, *49*, 2092–2120.
Dritschel, D. G., P. H. Haynes, and M. N. Juckes (1991), The stability of a two-dimensional vorticity filament under uniform strain, *J. Fluid Mech.*, *230*, 647–665.
Feldstein, S. B. (2003), The dynamics of NAO teleconnection pattern growth and decay, *Q. J. R. Meteorol. Soc.*, *129*, 901–924.
Fink, A. H., T. Brücher, E. Ermert, A. Krüger, and J. G. Pinto (2009), The European storm Kyrill in January 2007: Synoptic evolution, meteorological impacts and some considerations with respect to climate change, *Nat. Hazards Earth Syst. Sci.*, *9*, 405–423.
Franzke, C., S. Lee, and S. B. Feldstein (2004), Is the North Atlantic Oscillation a breaking wave?, *J. Atmos. Sci.*, *61*, 145–160.
Gabriel, A., and D. Peters (2008), A diagnostic study of different types of Rossby wave breaking events in the northern extratropics, *J. Meteorol. Soc. Jpn.*, *86*, 613–631.
Gómara, I., J. G. Pinto, T. Woollings, G. Masato, P. Zurita-Gotor, and B. Rodríguez-Fonseca (2014a), Rossby wave-breaking analysis of explosive cyclones in the Euro-Atlantic sector, *Q. J. R. Meteorol. Soc.*, *140*, 738–753, doi:10.1002/qj.2190.
Gómara, I., B. Rodríguez-Fonseca, P. Zurita-Gotor, and J. G. Pinto (2014b), On the relation between explosive cyclones affecting Europe and the North Atlantic Oscillation, *Geophys. Res. Lett.*, *41*, 2182–2190, doi:10.1002/2014GL059647.
Gyakum, J. R., and R. E. Danielson (2000), Analysis of meteorological precursors to ordinary and explosive cyclogenesis in the western North Pacific, *Mon. Weather Rev.*, *128*, 851–863.
Hanley, J., and R. Caballero (2012), The role of large-scale atmospheric flow and Rossby wave breaking in the evolution of extreme windstorms over Europe, *Geophys. Res. Lett.*, *39*, L21708, doi:10.1029/2012GL053408.
Hawcroft, M. K., L. C. Shaffrey, K. I. Hodges, and H. F. Dacre (2012), How much Northern Hemisphere precipitation is associated with extratropical cyclones?, *Geophys. Res. Lett.*, *39*, L24809, doi:10.1029/2012GL053866.
Haylock, M. R. (2011), European extra-tropical storm damage risk from a multimodel ensemble of dynamically-downscaled global climate models, *Nat. Hazards Earth Syst. Sci.*, *11*, 2847–2857.
Hewson, T. D. (1997), Objective identification of frontal wave cyclones, *Meteorol. Appl.*, *4*, 311–315.
Hewson, T. D. (1998), Objective fronts, *Meteorol. Appl.*, *5*, 37–65.
Hoskins, B. J., M. E. McIntyre, and A. W. Robertson (1985), On the use and significance of isentropic potential vorticity maps, *Q. J. R. Meteorol. Soc.*, *111*, 877–946.
Joly, A., and A. J. Thorpe (1990), Frontal instabilities generated by tropospheric potential vorticity anomalies, *Q. J. R. Meteorol. Soc.*, *116*, 525–560.
Joly, A., and A. J. Thorpe (1991), The stability of time-dependent flows: An application to fronts in developing baroclinic waves, *J. Atmos. Sci.*, *48*, 163–182.
Kalnay, E., et al. (1996), The NCEP/NCAR 40-Year Reanalysis Project, *Bull. Am. Meteorol. Soc.*, *77*, 437–471.
Karremann, M. K., J. G. Pinto, P. J. Von Bomhard, and M. Klawa (2014), On the clustering of winter storm loss events over Germany, *Nat. Hazards Earth Syst. Sci.*, *14*, 2041–2052.
Klawa, M., and U. Ulbrich (2003), A model for the estimation of storm losses and the identification of severe winter storms in Germany, *Nat. Hazards Earth Syst. Sci.*, *3*, 725–732.
Lamb, H. H. (1991), *Historic Storms of the North Sea, British Isles, and Northwest Europe*, Cambridge Univ. Press, Cambridge, U. K.
Mahlstein, I., O. Martius, C. Chevalier, and D. Ginsbourger (2012), Changes in the odds of extreme events in the Atlantic basin depending on the position of the extratropical jet, *Geophys. Res. Lett.*, *39*, L22805, doi:10.1029/2012GL053993.
Mailier, P. J., D. B. Stephenson, C. A. T. Ferro, and K. I. Hodges (2006), Serial clustering of extratropical cyclones, *Mon. Weather Rev.*, *134*, 2224–2240.
Masato, G., B. J. Hoskins, and T. Woollings (2013a), Wave-breaking characteristics of Northern Hemisphere winter blocking: A two-dimensional approach, *J. Clim.*, *26*, 4535–4549.
Masato, G., B. J. Hoskins, and T. Woollings (2013b), Winter and summer Northern Hemisphere blocking in CMIP5 models, *J. Clim.*, *26*, 7044–7059.
McCallum, E., and W. J. T. Norris (1990), The storms of January and February 1990, *Meteorol. Mag.*, *119*, 201–210.
McIntyre, M. E., and T. M. Palmer (1983), Breaking planetary waves in the stratosphere, *Nature*, *305*, 593–600.
Michel, C., and G. Rivière (2011), The link between Rossby wave breakings and weather regime transitions, *J. Atmos. Sci.*, *68*, 1730–1748.
Munich Re (2010), Significant European winter storms 1980−June 2010. Overall losses [in German]. [Available at www.munichre.com.]
Murray, R. J., and I. Simmonds (1991), A numerical scheme for tracking cyclone centres from digital data. Part I: Development and operation of the scheme, *Aust. Meteorol. Mag.*, *39*, 155–166.
Nakamura, H., and J. M. Wallace (1993), Synoptic behavior of baroclinic eddies during the blocking onset, *Mon. Weather Rev.*, *121*, 1892–1903.
Neu, U., et al. (2013), IMILAST—A community effort to intercompare extratropical cyclone detection and tracking algorithms, *Bull. Am. Meteorol. Soc.*, *94*, 529–547.
Orlanski, I. (2003), Bifurcation in eddy life cycles: Implications for storm track variability, *J. Atmos. Sci.*, *60*, 993–1023.
Parker, D. J. (1998), Secondary frontal waves in the North Atlantic region: A dynamical perspective of current ideas, *Q. J. R. Meteorol. Soc.*, *124*, 829–856.
Pelly, J. L., and B. J. Hoskins (2003), A new perspective on blocking, *J. Atmos. Sci.*, *60*, 743–755.
Pfahl, S., and H. Wernli (2012), Quantifying the relevance of cyclones for precipitation extremes, *J. Clim.*, *25*, 6770–6780.
Pinto, J. G., T. Spangehl, U. Ulbrich, and P. Speth (2005), Sensitivities of a cyclone detection and tracking algorithm: Individual tracks and climatology, *Meteorol. Z.*, *14*, 823–838.

Pinto, J. G., S. Zacharias, A. H. Fink, G. C. Leckebusch, and U. Ulbrich (2009), Factors contributing to the development of extreme North Atlantic cyclones and their relationship with the NAO, *Clim. Dyn.*, *32*, 711–737.
Pinto, J. G., N. Bellenbaum, M. K. Karremann, and P. M. Della-Marta (2013), Serial clustering of extratropical cyclones over the North Atlantic and Europe under recent and future climate conditions, *J. Geophys. Res. Atmos.*, *118*, 12,476–12,485, doi:10.1002/2013JD020564.
Plant, R. S., G. C. Craig, and S. L. Gray (2003), On a threefold classification of extratropical cyclogenesis, *Q. J. R. Meteorol. Soc.*, *129*, 2989–3012.
Raible, C. C. (2007), On the relation between extremes of midlatitude cyclones and the atmospheric circulation using ERA40, *Geophys. Res. Lett.*, *34*, L07703, doi:10.1029/2006GL029084.
Reed, R. J., and M. D. Albright (1986), A case study of explosive cyclogenesis in the eastern Pacific, *Mon. Weather Rev.*, *114*, 2297–2319.
Renfrew, I. A., A. J. Thorpe, and C. H. Bishop (1997), The role of the environmental flow in the development of secondary frontal cyclones, *Q. J. R. Meteorol. Soc.*, *123*, 1653–1675.
Riemer, M., S. C. Jones, and C. A. Davis (2008), The impact of extratropical transition on the downstream flow: An idealized modelling study with a straight jet, *Q. J. R. Meteorol. Soc.*, *134*, 69–91.
Rivals, H., J. P. Cammas, and I. A. Renfrew (1998), Secondary cyclogenesis: The initiation phase of a frontal wave observed over the eastern Atlantic, *Q. J. R. Meteorol. Soc.*, *124*, 243–267.
Rivière, G., and A. Joly (2006a), Role of the low-frequency deformation field on the explosive growth of extratropical cyclones at the jet exit. Part I: Barotropic critical region, *J. Atmos. Sci.*, *63*, 1965–1981.
Rivière, G., and A. Joly (2006b), Role of the low-frequency deformation field on the explosive growth of extratropical cyclones at the jet exit. Part II: Baroclinic critical region, *J. Atmos. Sci.*, *63*, 1982–1995.
Rivière, G., and I. Orlanski (2007), Characteristics of the Atlantic storm-track eddy activity and its relation with the North Atlantic Oscillation, *J. Atmos. Sci.*, *64*, 241–266.
Rudeva, I., and S. K. Gulev (2007), Climatology of cyclone size characteristics and their changes during the cyclone life cycle, *Mon. Weather Rev.*, *135*, 2568–2587.
Schär, C., and H. C. Davies (1990), An instability of mature cold fronts, *J. Atmos. Sci.*, *47*, 929–950.
Schwierz, C., et al. (2010), Modelling European winter wind storm losses in current and future climate, *Clim. Change*, *101*, 485–514.
Shaffrey, L. C., et al. (2009), UK-HiGEM: The new UK High Resolution Global Environment Model. Model description and basic evaluation, *J. Clim.*, *22*, 1861–1896.
Simmonds, I. (2000), Size changes over the life of sea level cyclones in the NCEP reanalysis, *Mon. Weather Rev.*, *128*, 4118–4125.
Simmonds, I., and K. Keay (2000), Mean Southern Hemisphere extratropical cyclone behavior in the 40-year NCEP–NCAR reanalysis, *J. Clim.*, *13*, 873–885.
Simmons, A. J., and B. J. Hoskins (1979), The downstream and upstream development of unstable baroclinic waves, *J. Atmos. Sci.*, *36*, 1239–1254.
Strong, C., and G. Magnusdottir (2008a), How Rossby wave breaking over the Pacific forces the North Atlantic Oscillation, *Geophys. Res. Lett.*, *35*, L10706, doi:10.1029/2008GL033578.
Strong, C., and G. Magnusdottir (2008b), Tropospheric Rossby wave breaking and the NAO/NAM, *J. Atmos. Sci.*, *65*, 2861–2876.
Thorncroft, C. D., B. J. Hoskins, and M. E. McIntyre (1993), Two paradigms of baroclinic-wave life-cycle behaviour, *Q. J. R. Meteorol. Soc.*, *119*, 17–55.
Uccellini, L. W. (1990), Processes contributing to the rapid development of extratropical cyclones, in *Extratropical Cyclones: The Erik Palmen Memorial Volume*, edited by C. Newton and E. O. Holopainen, pp. 81–105, Am. Meteorol. Soc., Boston, Mass.
Ulbrich, U., A. H. Fink, M. Klawa, and J. G. Pinto (2001), Three extreme storms over Europe in December 1999, *Weather*, *56*, 70–80.
Vitolo, R., D. B. Stephenson, I. M. Cook, and K. Mitchell-Wallace (2009), Serial clustering of intense European storms, *Meteorol. Z.*, *18*, 411–424.
Woollings, T., A. Hannachi, and B. Hoskins (2010), Variability of the North Atlantic eddy-driven jet stream, *Q. J. R. Meteorol. Soc.*, *136*, 856–868.